Applied Catalysis B: Environmental 160–161 (2014) 506–513

Contents lists available at ScienceDirect

Applied Catalysis B: Environmental

journal homepage: www.elsevier.com/locate/apcatb

Semi-pilot scale environment friendly photocatalytic degradation of 4-chlorophenol with singlet oxygen species—Direct comparison with H_2O_2/UV-C reaction system

Pavel Krystynik[a,*], Petr Kluson[a,b], Stanislav Hejda[b], Daniel Buzek[b], Pavel Masin[c], Duarte Novaes Tito[d]

[a] Institute of Chemical Process Fundamentals, Academy of Sciences of the Czech Republic, Rozvojova 135, 165 02 Prague 6, Czech Republic
[b] Faculty of Environment, University of J.E. Purkyne, Kralova vysina 18, Usti nad Labem 560 04, Czech Republic
[c] Dekonta a.s., Volutova 2523, 158 00 Prague, Czech Republic
[d] Elysium Projects, Stanton, LL59 5PE, Menai Bridge UK

ARTICLE INFO

Article history:
Received 8 April 2014
Received in revised form 23 May 2014
Accepted 29 May 2014
Available online 5 June 2014

Keywords:
Phthalocyanine
Photocatalysis
Photochemical oxidation
Singlet oxygen
Hydrogen peroxide
UV-C/H_2O_2
Water treatment

ABSTRACT

Metal phthalocyanines in the presence of visible light are applied in the semi-pilot level for the degradation of organic pollution represented by 4-chlorophenol (4-CP) with potential further scale-up. The effectiveness of the process based on the generation of singlet oxygen active species is compared with commonly used method of photochemical oxidation with hydrogen peroxide in the presence of ultraviolet irradiation. The direct comparison of the reaction systems was conceivable because both oxidation processes were carried out in identical experimental arrangements and under identical reaction conditions. The comparison was performed in terms of 4-CP conversion, TOC removal, apparent quantum yields, kinetic constants, and economy considerations. It must be emphasized there have been no reports on the semi pilot scale utilization of phthalocyanines for decontamination purposes previously.

1. Introduction

Occurrence of trace organics in wastewaters is a serious problem throughout the world. Their release from industrial plants of various types is the major source. Some part of the involved organics is non-biodegradable and conventional treatment methods fail [1]. A possible option is to employ highly reactive oxidative species such as singlet oxygen or hydroxyl radicals. Singlet oxygen can be generated by photosensitive compounds via their interaction with light of appropriate wavelength [2–4]. Hydroxyl radicals can be generated by means of various processes. The most common source is hydrogen peroxide [5,6]. In this communication we report on continuation of our recent research on metal phthalocyanines (PC) as efficient photocatalysts [7–9]. Here the metal PCs are applied in the semi-pilot level for the degradation of organic pollution represented by 4-chlorophenol with potential further scale-up. The effectiveness of this process was compared with commonly used method of photochemical oxidation with hydrogen peroxide in the presence of ultraviolet irradiation. The direct comparison of the reaction systems was conceivable because both oxidation processes were carried out in identical experimental arrangements and under identical reaction conditions (with exception of light emission fields).

Singlet oxygen can be efficiently generated by various types of PCs. These molecules contain the tetrapyrrole structure similarly to hem or chlorophyll (Fig. 1). They form complexes with many metals and metalloids, however, the most commonly used are copper, zinc, and aluminum phthalocyanines [10–12]. PCs' low solubility limits their practical applicability, modifications through halogenation, chlorine methylation, sulfonation or sulfochlorination is thus necessary.

The general mechanism of the phthalocyanine interaction with light is usually described by two types of reaction mechanisms [13–15]. It starts with its absorption of photon(s) followed by intersystem crossing from the excited singlet state to the low-lying triplet state. The triplet state of phthalocyanine transfers its energy to an oxygen molecule. More detailed view on phthalocyanine excitation mechanisms can be found elsewhere [16–18]. The simplified

* Corresponding author. Tel.: +420 220 390 278.
E-mail address: krystynik@icpf.cas.cz (P. Krystynik).

http://dx.doi.org/10.1016/j.apcatb.2014.05.051
0926-3373/

Nomenclature

4-CP	4-chlorophenol
ZnPC	zinc phthalocyanine
AOPs	advanced oxidation processes
TOC	total organic carbon
HPLC	high performance liquid chromatography
UV	ultraviolet
VIS	visible
NIR	near infrared
UV-C/H_2O_2	reaction system using hydrogen peroxide and shortwave ultraviolet irradiation
VIS/ZnPC	reaction system using visible light and zinc phthalocyanine
c_A	concentration of reactant (mmol l^{-1})
t	reaction time
c_{A0}	initial concentration of reactant (mmol l^{-1})
k	rate constant (s^{-1})
n	order of reaction
b_t	sequence of approximates
S	minimizing value of objective function
b_0	initial parameter estimates
d	normalized random vector
l	random step
RND	random Number from interval (0; 1)
n_{tot}	number of random selections
n_{succ}	number if selections leading to better estimates
R	allowable search region
I	current (A)
P_f	irradiation intensity (W cm^{-2})
E	voltage measured (V)
R	selected resistance (Ω)
s	detector photosensitivity at specific wavelengths (A W^{-1})
H	illuminated area of detector
λ	wavelength of light (nm)
h	Planck constant = 6.626×10^{-34} J s
N_A	Avogadro's number = 6.022×10^{23}
$J_{h\nu}$	Photon flux intensity (Einstein s^{-1} cm^{-1})
$\Phi_{4\text{-CP}}$	apparent quantum yield
V	reaction volume (cm^3)
$c_{4\text{-CP}}$	Initial concentration of 4-CP (mmol l^{-1})
A	Illuminated area of reaction (cm^2)

mechanism of singlet oxygen generation is described by the scheme (1):

$$PC + h\nu \rightarrow {}^1PC*(+isc) \rightarrow {}^3PC* \rightarrow {}^1O_2 \quad (1)$$

The UV-C/H_2O_2 system is based on the decomposition of hydrogen peroxide towards hydroxyl radicals using ultraviolet irradiation with wavelengths below 280 nm [19]. The mechanism of hydroxyl radical formation is understood as homolytic cleavage of hydrogen peroxide molecule yielding two radicals.

$$H_2O_2 + h\nu \rightarrow 2OH^{\bullet} \quad (2)$$

In aqueous environment the cage effect of water molecules decreases the quantum yield of radical generation to 0.5 [20]. On the contrary hydrogen peroxide has a small absorption coefficient (18.6 M^{-1} cm^{-1} at 254 nm), thus the utilization of UV-C light source is decreased when organic compounds act as optical filters. More details on the mechanism of hydrogen peroxide decomposition can be found elsewhere [21–23].

In this paper we report on the comparison of two semi-pilot scale reactor systems using singlet oxygen generated by ZnPC

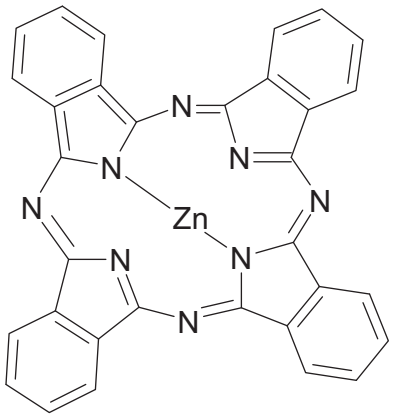

Fig. 1. Phthalocyanine molecule with central Zn atom.

(Fig. 1) upon its visible light illumination, and hydroxyl radicals formed by direct photolysis (UV-C) of hydrogen peroxide. This comparison was feasible due to the construction of two reaction units of identical design and scale. To the best of our knowledge such direct comparison has never been reported. Also, there have been no reports on the semi pilot scale utilization of phthalocyanines for decontamination purposes.

2. Experimental

2.1. Chemicals

4-Chlorophenol (per analysis quality, Sigma–Aldrich), sulfonated ZnPC (per analysis quality, prepared according to [24]) and 30% solution of hydrogen peroxide (per analysis quality, Lach-Ner) were used. 4-Chlorophenol solutions were prepared with deionized water (conductivity below 1 μS cm^{-1}). Sodium hydroxide (per analysis quality, Lach-Ner) was used for the pH adjustment during experiments with PC.

2.2. The reactors

Both photochemical reaction units were built as tubular reactors with recirculation loops. The reactors are self-designed and in-house developed with arrangements as shown in Fig. 2. Despite the reaction systems were of identical there were inevitable subtle differences in the photoreactor part.

Contaminated water from the storage tank (1) is pumped with centrifugal pump (2) to the photoreactor (6). While passing through the photoreactor it is irradiated and then it is brought back to the storage tank through the heat exchanger to ensure the isothermal regime. There are also other parts: membrane valve (3) for the control of the flow rate, flow-meter (4), sampling valve (7) and the bypass (5) for blank experiments or homogenization of the reaction mixture. The hydrogen peroxide dispenser (8) can be connected with help of a mixing valve (9) ensuring homogeneous reaction mixture before entering the photoreactor. For VIS/ZnPC experiments the hydrogen peroxide dispenser is replaced with the NaOH solution dispenser.

On Fig. 3 the *x*-cross section of the photoreactor with all important dimensions can be seen. Both reactors were of similar construction, with differences in length as depicted in the figure. The central reactors' tube is surrounded with lamps emitting at relevant wavelengths. The VIS photoreactor is made from standard glass tube (570 mm long, 56 mm wide-inner diameter) surrounded by 12 lamps emitting at 630–670 nm (Philips, TL-D 18W Red 1PP). The UV-C photoreactor consists of a quartz tube (290 mm long, 56 mm wide-inner diameter) surrounded by 12 germicidal

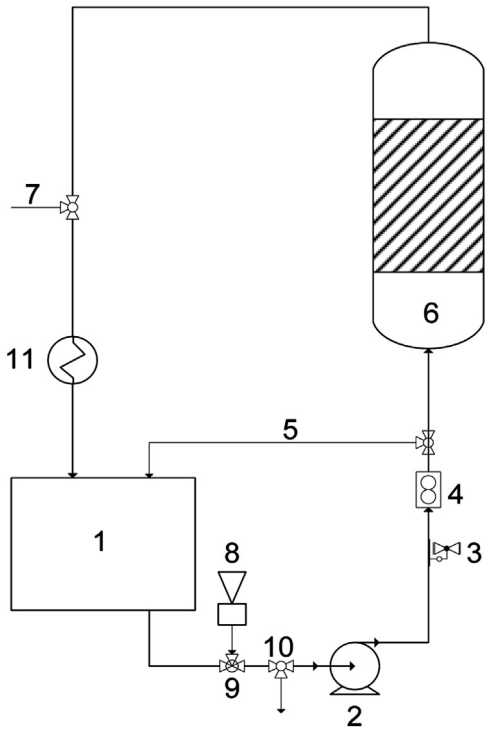

Fig. 2. Sketch of the experimental set-up: (1) storage tank, (2) centrifugal pump, (3) membrane valve, (4) flow meter, (5) by pass, (6) photoreactor, (7) sampling, (8) hydrogen peroxide storage tank, (9) mixing valve, (10) outlet valve, (11) heat exchanger.

low-pressure UV lamps with maximum emission at 254 nm (Philips, LT 8W UV-C). Reactor outer jackets are made of highly polished aluminum sheet to ensure maximum light reflectance including lengthwise sheets to conduct the produced heat away. The process temperature was maintained by a cooling coil located inside the storage tank at 25 °C. The photoreactors' inlet comprised a re-distributor and series of sieves to ensure the uniform flow through the irradiated zone. In the UV-C reactor system all inner parts were made of plastic to prevent hydrogen peroxide decomposition induced by metal parts.

2.3. Typical experiment

Initial concentration of 4-chlorophenol (4-CP) was usually 0.5 mmol l^{-1}. Other used concentrations are specified further in the text. The concentration of ZnPC was typically 0.01 mmol l^{-1}, hydrogen peroxide was dosed with concentration of 2.5 mmol l^{-1} h^{-1}. Reaction mixture volume was usually 40 l, however, the system's capacity was 100 l. The typical reaction time was 300 min. The reaction mixture was always homogenized first by recirculation using the by-pass for 10 min with flow rate 25 l min^{-1}. After this step the UV lamps were turned on and the automated dosing of NaOH or H_2O_2 was switched on. The dosing point was positioned just before the reaction mixture entered the centrifugal pump to ensure its homogeneity. The sampling probe was located in a mixing valve in front of a centrifugal pump as shown in Fig. 2. The necessity of NaOH dosage was discussed elsewhere [9].

2.4. Analytical

The parameter of TOC (total organic carbon) was followed with TOC analyzer Shimadzu TOC-Vwp. The method is based on the photolysis of sodium persulfate and additional oxidation by the produced sulfate radical-anions. Total organic carbon is calculated as the difference of total and inorganic carbon. Light absorption changes of samples of reaction mixtures were measured with a Perkin Elmer UV/VIS/NIR spectrometer Lambda 19 from 200 to 800 nm. An HPLC chromatographer DIONEX UltiMate 3000 Series equipped with TCC-3000 SD column and DAD detector was used for determination of 4-CP concentration. Analytical conditions: temperature was 30 °C, mobile phase consisted of 70% of methanol and 30% of deionized water, the flow-rate was set up to 1 ml min^{-1}.

2.5. Kinetic data evaluation

For kinetic data evaluation a simple differential equation was used:

$$-\frac{dc_A}{d\tau} = k \cdot c_A^n \quad (3)$$

It was converted to integral proportions where concentration of reactant is a function of time:

$$c_A = c_{A0} \cdot [1 + (n-1) \cdot c_{A0}^{n-1} \cdot k \cdot t]^{1/(n-1)} \quad (4)$$

c_A is the concentration of reactant in time t, c_{A0} is the initial reactant concentration, k is the rate constant and n is the reaction order.

For the regression analysis the ERA software was used [25]. The software covers parameters' estimation, reliability, significance and residual distribution tests, covariance tests and design of experiments. Parameters' estimation is based on the best fit of experimental data according to chosen optima criterion. A brief random search algorithm is given in Fig. 4.

Symbols in Fig. 4 have following relevance: b_t is the sequence of approximations, minimizing value of objective function S, is generated with initial parameter estimates b_0. Vector d is normalized random vector, the elements of which were sampled from interval $(-1; 1)$. l is random step. Random step length l is chosen according to the equation (5):

$$l = R(\mathrm{RND})^{\ln(n_{tot}/n_{succ})} \quad (5)$$

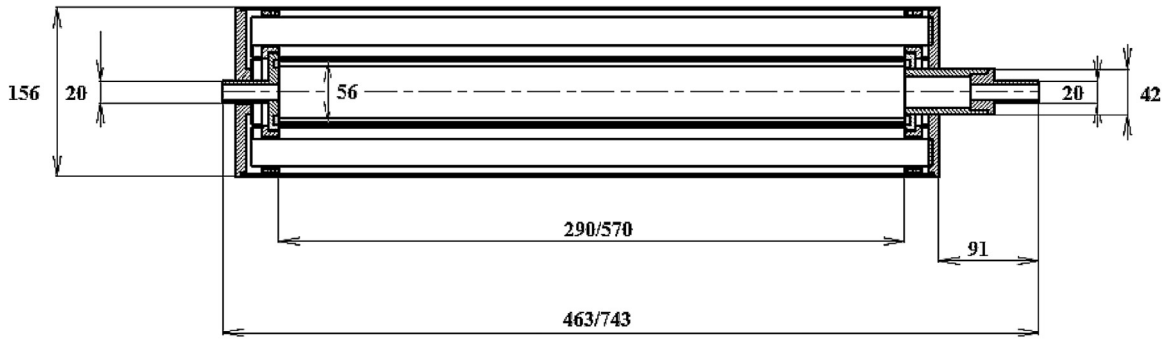

Fig. 3. The sectional view on photoreactor construction with dimensions (mm).

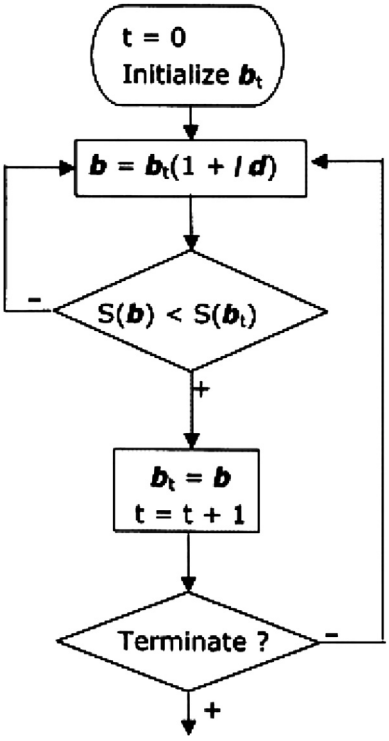

Fig. 4. The algorithm used to obtain the kinetic constants; b_t is sequence of approximations, S minimizing value of objective function, b_0 initial parameter estimates, d normalized random vector, l is random step. Random step l is taken from the equation 10.

RND is a random number from interval (0; 1), n_{tot} number of random selections, n_{succ} number of selections leading to better estimates and R allowable search region. Parameters d and l are generated uniquely in every iteration step. Random step length uses a variable distribution of random numbers to ensure a reliable convergence to the global optimum and a reasonable convergence speed.

Apparent quantum yields are determined as yield of the photodegradation of 4-CP ($\Phi_{4\text{-CP}}$) [9]. For calculations of apparent quantum yields it is necessary to determine the intensity of irradiation P_f, and the reaction rate constant k,

$$P_f = \frac{I}{s \cdot H} = \frac{E}{R \cdot s \cdot H} \quad (6)$$

where I is the current (A), P_f irradiation intensity (W cm^{-2}), E voltage measured (V), R selected resistance (Ω), s detector photosensitivity at specific wavelengths (A W^{-1}) and H illuminated area of detector = 1 cm^2. Values of s are given by the detector provider. The intensity was measured by radiometer (Multimeter M3850D, Metex; Si photodiode Hamamatsu S1337-BQ, detector 1 cm × 1 cm). Then it is necessary to determine the photon flux intensity ($J_{h\nu}$),

$$J_{h\nu} = \frac{\lambda \cdot P_f}{h \cdot \gamma \cdot N_A} \quad (7)$$

where λ is the wavelength of light (nm), Planck constant $h = 6.626 \times 10^{-34}$ Js, N_A is Avogadro's number 6.022×10^{23}. $J_{h\nu}$ can be expressed in units of Einstein s^{-1} cm^{-1}, where 1 Einstein = 1 mol of photons. Using the rate constant and photon flux intensity the apparent quantum yield $\Phi_{4\text{-CP}}$ can be calculated:

$$\Phi_{4\text{-CP}} = \frac{V \cdot c_{4\text{-CP}} \cdot k}{J_{h\nu} \cdot A} \cdot 100\% \quad (8)$$

Table 1
Standard reduction potentials for a series of oxidizing agents [26].

Oxidizing agent	Reaction	E [V]
Fluorine	$F_2 + 2H^+ + 2e^- \rightleftharpoons 2HF$ (aq)	3.03
Hydroxyl radical	**$OH\bullet + H^+ + e^- \rightleftharpoons H_2O$**	**2.8**
Singlet oxygen	**$^1O_2 + 2H^+ + 2e^- \rightleftharpoons H_2O$**	**2.42**
Ozone	$O_3 + 2H^+ + 2e^- \rightleftharpoons H_2O + O_2$	2.07
Sodium peroxodisulfate	$S_2O_8^{2-} + 2e^- \rightleftharpoons 2SO_4^{2-}$	2.01
Hydrogen peroxide	$H_2O_2 + 2H^+ + 2e^- \rightleftharpoons 2H_2O + O_2$	1.78
Hydroperoxide radical	$2HO_2\bullet + 2H^+ + 2e^- \rightleftharpoons 2H_2O + O_2$	1.7
Potassium permanganate	$MnO_4^- + 8H^+ + 5e^- \rightleftharpoons Mn^{2+} + 4H_2O$	1.68
Chlorine dioxide	$ClO_2 + 4H^+ + 5e^- \rightleftharpoons Cl^- + 2H_2O$	1.57
Potassium dichromate	$Cr_2O_7^{2-} + 14H^+ + 6e^- \rightleftharpoons 2Cr^{3+} + 7H_2O$	1.38
Chlorine	$Cl_2 + 2e^- \rightleftharpoons 2Cl^-$	1.36
Dissolved oxygen	O_2 (g) $+ 4H^+ + 4e^- \rightleftharpoons 2H_2O$	1.22

in which V is a reaction volume (cm^3), $c_{4\text{-CP}}$ initial concentration of 4-CP, k is a rate constant (s^{-1}) and A is the illuminated area of reaction (cm^2).

3. Results and discussion

Two reactive oxidizing agents, singlet oxygen and hydroxyl radicals, were compared in terms of their efficacy toward the degradation of 4-CP in semi-pilot scale. In Table 1 we can inspect the most common oxidizing agents arranged according to their standard reduction potentials [26]. Hydroxyl radical and singlet oxygen are on the second and the third positions, respectively.

3.1. Blank experiments

The stability of ZnPC was tested by irradiating the ZnPC solution without 4-CP. It was observed that ZnPC was stable during the period of 10 h of irradiation in the VIS region. The stability of UV-C/H_2O_2 system was tested by decomposition of H_2O_2 in deionized water also without 4-CP. This experiment was performed periodically and it was assumed as test of the internal integrity of the system. Direct degradation of 4-CP under lamps emitting mainly in visible area without ZnPC, and reaction of ZnPC with 4-CP under dark conditions were carried out. Also direct degradation of 4-CP by UV-C photolysis, and its oxidation with H_2O_2 in the dark were inspected.

Fig. 5 refers to the blank experiments for both reaction systems as it is mentioned in the legend. The highest conversion of 4-CP can

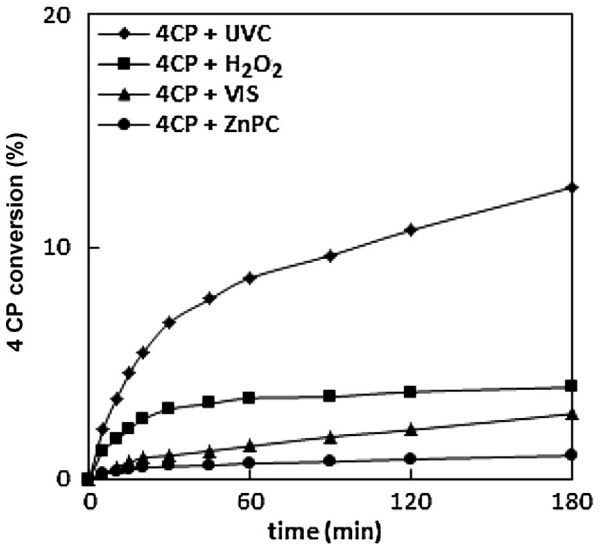

Fig. 5. Comparison of 4-CP degradation for the series of blank experiments.

be observed for the direct photolysis induced by UV-C irradiation at 254 nm. The achieved conversion was ~12% after 180 min. Much lower conversion of 4% was observed when 4-CP was oxidized with hydrogen peroxide without the UV-C irradiation. Hydrogen peroxide belongs to oxidizing agents and it is capable of partial oxidation of 4-CP (see Table 1). The lowest conversion of 4-CP (less than 1%) was observed when employing ZnPC under dark conditions. The PC itself is incapable of 4-CP oxidation because no photons were introduced thus the singlet oxygen could not be generated (the ~1% conversion can be referred to as analytical error). Direct photolysis of 4-CP, without ZnPC, achieved a conversion level of ~2%. That is due to full emission spectra of the lamps. The main irradiation peak is located at 630–670 nm, however minor emitting peak can be found in the UV area and this is responsible for the minor 4-CP direct photolysis.

3.2. Optimization experiments

Once blank experiments were performed, it was necessary to carry out a series of optimization tests. These were based on inspecting the sensitivity of both reaction systems to various process parameters (flow rate, intensity of irradiation, concentration of ZnPC, H_2O_2, reaction mixture volume). All the optimized parameters can be found in Table 2.

The flow rate range was determined by the maximum pump output (25 l min^{-1}) whilst the minimum was set by the flow rate required to prevent clogging of the pump (5 l min^{-1}). However, the flow rate range was limited by the type of pump. It was determined that the flow rate revealed only negligible influence on the reaction rates and the achieved apparent quantum yields.

The intensity of irradiation was varied by controlling the number of lamps under operation (2 to 12, 8 lamps were identified as optimal). The reaction mixture volume was optimized to 40 l and the initial 4-CP concentration was 0.5 mmol l^{-1} (~59 ppm of TOC). It must be emphasized that both reaction systems allowed operations up to the reaction volume 100 l.

Optimal concentration of ZnPC was determined at 0.01 mmol l^{-1}. Lower ZnPC concentrations lead to lower reaction rates whilst higher concentrations lead to dark blue coloring of the reaction mixture. Dark blue color prevented an effective contact of light with the PC in the whole volume of the reaction mixture. It was found that the darker the solution was the lower was the observed reaction rate because the solution itself acted as an optical filter. Concentration of hydrogen peroxide 12.5 mmol l^{-1} and 300 min of the residence time were identified as optimal. The reaction rate was also very low at neutral pH. The optimal pH value was determined at 10 [12].

The level of the phthalocyanine concentration was optimized to achieve the highest reaction rate. The finally used concentration (0.01 mmol l^{-1}) was the limit above which the reaction did not already proceed at higher rates.

The concentration employed for hydrogen peroxide reflects more inputting variables. It must be emphasized that the overall economy balance was the major indicator. It included the amount of consumed hydrogen peroxide, its concentration, rate of dosing, and obviously also the energy used for its photochemical splitting. The tested concentration range for hydrogen peroxide was 1–15 mmol l^{-1} h^{-1}. Higher concentration (above the optimal level) may comprise the reaction rate increase, but due to its price, and more energy needed for its photoinduced reactions, it leads to higher cost per one processed liter of water.

3.3. Comparison tests/UV–VIS

In Fig. 6 on the left, we can observe absorption changes for the VIS/ZnPC system plotted as function of time. It can be seen again the main absorption peaks below 300 nm progressively change during the reaction into one main maximum outside the plotted area indicating the formation of reaction intermediates. The decrease of absorbance below 300 nm was not achieved. The two characteristic absorption bands at 630 and 680 nm could be assigned to the dimmer and monomer of ZnPC, respectively [8]. They evidence for sufficient stability of the used ZnPC under experimental conditions.

Similar changes of absorption spectra can be observed also on the right part of Fig. 6 referring to the UV-C/H_2O_2 reaction system. We can recognize the main characteristic absorption maxima below 300 nm, namely at 200, 220 and 280 nm at the beginning of reaction. As the reaction progressed it was obvious that all the absorption peaks were decreasing. The secondary increase of absorption at 250 nm with maximum outside the plotted area indicated formation of reaction intermediates. As they were progressively decomposed their absorbance was also decreasing.

Fig. 7 shows the effect of 4-CP initial concentration. The left part describes it again for the VIS/ZnPC system with constant concentration of ZnPC, namely 1×10^{-5} mol l^{-1}. The highest conversion for 4-CP oxidation, and nearly complete removal (94%) after reaction time of 300 min, was found for the starting concentration of 0.5 mmol l^{-1}. Higher concentrations of 1 mmol l^{-1}, 1.5 mmol l^{-1}, and 2 mmol l^{-1} reveal conversions of 56%, 42% and 28%, respectively therefore the reaction time needed for 4-CP complete removal will be significantly higher.

On the right the influence of 4-CP initial concentration on its removal rate for UV-C/H_2O_2 system is shown. The H_2O_2 dosing rate (30% solution) was kept constant at 2.5 mmol l^{-1} h^{-1}. The reaction time needed for oxidation of 4-CP increased progressively with its increasing concentration. Complete 4-CP oxidation was achieved in 60 min for the initial concentration of 0.5 mmol l^{-1}. For concentrations 1 mmol l^{-1}, 1.5 mmol l^{-1}, and 2 mmol l^{-1} the reaction times needed to be raised to 120 min, 150 min, and 180 min, respectively in order to achieve complete 4-CP conversion. Lower reaction rates at higher concentrations could be attributed to the competition among 4-CP molecules and many reaction intermediates for the generated active species ($OH^{\bullet}$ and $^1O_2$) [27].

3.4. Comparison tests/TOC

Both chosen methods use strong oxidizing agents capable to mineralize 4-CP and reaction intermediates to H_2O, CO_2, and HCl. Left part of Fig. 8 shows degree of TOC removal for various initial TOC content for VIS/ZnPC system. It is obvious that increasing initial TOC content lead to lower degree of TOC removal. Observed degrees of TOC removal were 29%, 21%, 15% and 10% for initial contents of 59 mg l^{-1}, 119 mg l^{-1}, 165 mg l^{-1} and 222 mg l^{-1}, respectively. Lower efficiency of the TOC removal was expected because the corresponding 4-CP conversions (Fig. 7) for the ZnPC system were identified lower than for UV-C/H_2O_2 system. The degree of TOC removal for higher concentrations appeared to be sensitive to initial TOC concentration. The formation of oxidative species seemed to be decreasing by increasing the initial TOC content. With higher concentration of reaction intermediates less portion of light would be available for the oxidative species generation.

Right part of Fig. 8 shows corresponding degrees of TOC removal for the UV-C/H_2O_2 system. It is obvious that for initial TOC content of 59 mg l^{-1} a 100% degree of removal was achieved during the reaction time of 300 min but more than 95% conversion was observed after 180 min of the experimental run. Higher levels indicate lower degrees of TOC removal: concentration of 119 mg l^{-1} reveals about 78%, 165 mg l^{-1} and 222 mg l^{-1} show 55% and 32%, respectively. TOC removal is mainly dependent on the H_2O_2 dosage. It can be considered that higher degree of TOC removal would be achieved with prolonged reaction time and higher dosing rate. It is obvious

Table 2
Summary of optimization experiments.

Parameter	Optimization range	ZnPC/VIS system Optimized values	UV-C/H_2O_2 system Optimized values
Flow rate	5–25 l min^{-1}	25 l min^{-1}	25 l min^{-1}
Intensity of irradiation	180–1080 mW cm^{-2} 150–900 mW cm^{-2}	600 mW cm^{-2}	720 mW cm^{-2}
Reaction mixture volume	10–100 l	40 l	40 l
4-CP initial concentration	0.1–2 mmol l^{-1}	0.5 mmol l^{-1}	0.5 mmol l^{-1}
H_2O_2 concentration	1–15 mmol l^{-1} h^{-1}	n/a	2.5 mmol l^{-1} h^{-1}
pH of reaction solution	7–12	10	n/a
ZnPC concentration	0.0001–1 mmol l^{-1}	0.01 mmol l^{-1}	n/a

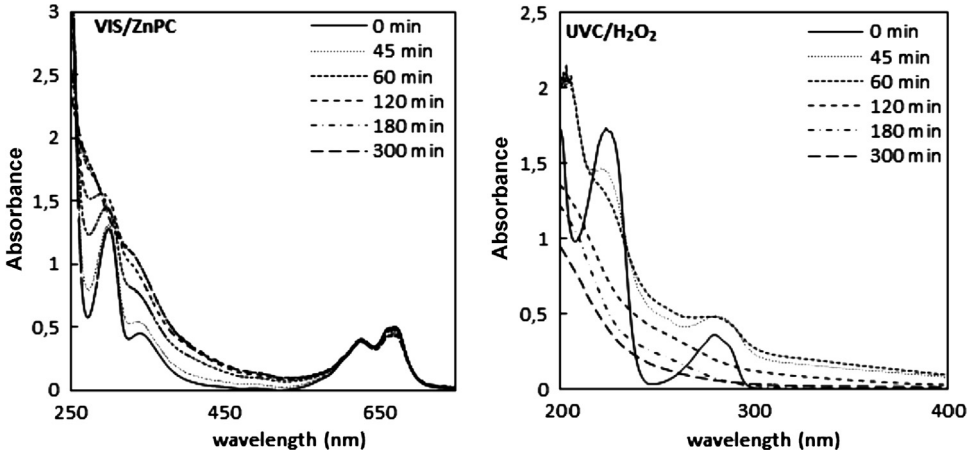

Fig. 6. Comparison of spectral changes.

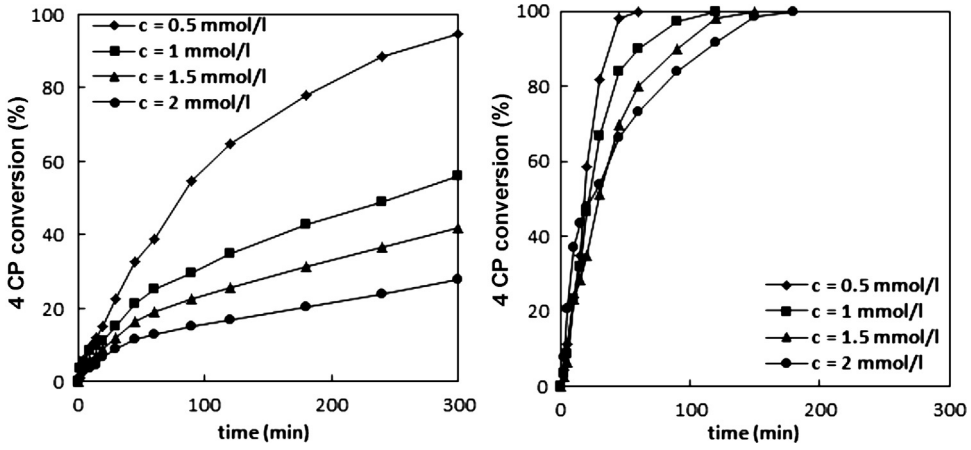

Fig. 7. The influence of 4-CP initial concentration; left – degradation with constant ZnPC concentration, right – degradation with constant H_2O_2 continuous dosing.

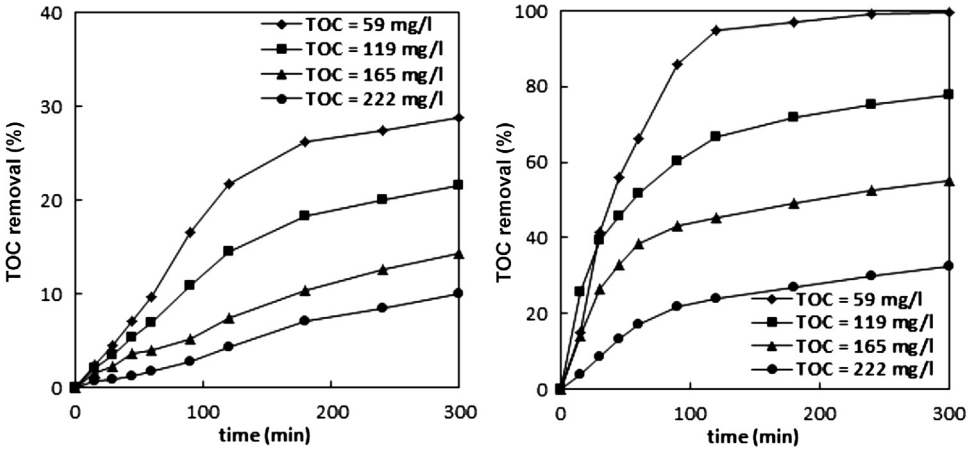

Fig. 8. The influence of initial TOC; left – VIS/ZnPC system, right – UV-C/H_2O_2 system.

Table 3
Rate constants and apparent quantum yields.

4-CP concentration (mmol l^{-1})	VIS/ZnPC system		UV-C/H_2O_2 system	
	Rate constant (s^{-1})	Apparent quantum yield (%)	Rate constant (s^{-1})	Apparent quantum yield (%)
0.5	0.015	0.054	0.141	0.516
1	0.016	0.058	0.076	0.278
1.5	0.013	0.047	0.068	0.249
2	0.009	0.043	0.039	0.142

Table 4
Economical balance estimations.

	VIS/ZnPC system		UV-C/H_2O_2 system	
	Consumption per 1 m^3 of water	Price [EUR] per 1 m^3 of water	Consumption per 1 m^3 of water	Price [EUR] per 1 m^3 of water
Electricity	75 kWh	11.54	10 kWh	1.53
Hydrogen peroxide	n/a	n/a	1000 ml	0.35
Zn Phthalocyanine	4.1 kg	0.47	n/a	n/a
Photoreactor maintenance		0.02		0.08
Operating cost		12.03		1.96

that UV-C/H_2O_2 system reveals significantly higher efficiency in TOC removal.

It should be emphasized again the technologies are identical regarding their constructions, hydrodynamics, sampling, data evaluation, etc. In the first one (VIS/ZnPC) visible light is used to produce singlet oxygen species. They are very reactive, but of course, also very different from the species generated by direct hydrogen peroxide UV-C photolysis (the second system). However, we do believe that due to careful optimization the systems are in the overall sense comparable.

3.5. Kinetic analysis and apparent quantum yields

The kinetics of 4-CP oxidation was determined with respect to optimized conditions. Rate constants were calculated according the equations (3) and (4), apparent quantum yields were evaluated using equations (7) and (8). Reaction of chlorophenols with hydroxyl radicals and singlet oxygen are usually described with pseudo-first order kinetics [28–31]. Experimental data fitted the pseudo-first reaction model satisfactorily ($p < 0.05$) using the ERA software. The kinetic data are summarized in Table 3.

In the UV-C/H_2O_2 system we could observe that the rate constant was systematically decreasing with increasing the initial concentration of 4-CP, while hydrogen peroxide dosing rate was kept at the constant level. The decreasing value of the rate constant indicates better utilization of hydroxyl radicals for oxidations, thus side reactions occur at less extent. Obviously higher rate constant would be observed with higher H_2O_2 dosing rate. The VIS/ZnPC system reveals lower rate constants and lower apparent quantum yields. These findings are consistent with lower 4-CP conversion and lower TOC removal during the oxidation process. The rate constants and apparent quantum yields also reveal some decreasing tendency within the tested range of initial 4-CP concentration as observed in the UV-C/H_2O_2 system.

The economy balance of water treatment in both oxidation units is based on rough estimation of energy consumption for lamps and pump supply, and costs of the used chemicals. The price is calculated for the contaminated water with concentration of 55 mg l^{-1} containing TOC, mainly from 4-CP contamination. The used price of electricity is 0.15 EUR/kWh. The unit costs of electricity for both technologies are identical. The total price of electricity is significantly higher for VIS/ZnPC system because longer reaction time is needed for effective treatment of contaminated water. Price of ZnPC is 0.12 EUR per gram. The total process cost of decontamination using VIS/ZnPC unit is 12.03 EUR per 1 m^3 of contaminated water. The wholesale price of hydrogen peroxide solution (35%) is 0.35 EUR per liter. That total process cost in this system is 1.96 EUR per 1 m^3 of contaminated water. The difference is clearly evident (Table 4).

4. Conclusion

Photocatalytic degradations of 4-chlorophenol in VIS/ZnPC semi-pilot scale system was studied. For these purposes a reaction unit was designed and constructed as tubular reactor working in differential mode. The system optimization was carried out and the process was compared with the commonly used technology utilizing UV-C/H_2O_2, and carried out in identical technical arrangement. The comparison of optimized processes was performed for several indicators: 4-CP conversion, degree of TOC removal, rate constants, apparent quantum yields and economical evaluation. 4-CP conversion and TOC removal is highly dependent on PC concentration, as well as on H_2O_2 concentration and both indicators showed lower efficiency for the VIS/ZnPC system. Rate constants and apparent quantum yields are 4-CP concentration sensitive and systematically decrease with increasing the 4-CP concentration. For these indicators, VIS/ZnPC system showed again lower values; rate constant is approx. 10 times lower. Operating cost is significantly higher for VIS/ZnPC system as consequence of low reaction rate and higher time needed for the total oxidation of 4-CP.

Acknowledgement

Financial support of Technology Agency of the Czech Republic (project no. TA03010548) is gratefully acknowledged. Additional financial support from the ECOP (The Education for Competitiveness Operational Programme; Grant No. CZ.1.07/2.2.00/28.0205) and from the Internal Grant Agency of the University of Jan Evangelista Purkyne in Usti nad Labem is gratefully acknowledged.

References

[1] S.M. Borghei, S.N. Hosseini, Chem. Eng. J. 139 (2005) 482–488.
[2] J. Cerny, M. Karaskova, J. Rakusan, S. Nespurek, J. Photochem. Photobiol. A: Chem. 210 (2010) 82–88.
[3] M.D. Maree, N. Kuznetsova, T. Nyokong, J. Photochem. Photobiol. A: Chem. 140 (2001) 117–125.
[4] A.B. Ormond, H.S. Freeman, Dyes Pigm. 96 (2013) 440–448.
[5] M.Y. Ghaly, G. Härtel, R. Mayer, R. Haseneder, Waste Manage. 21 (2001) 41–47.
[6] A.A. Burbano, D.D. Dionysiou, M.T. Suidan, T.L. Richardson, Water Res. 39 (2005) 107–118.

[7] P. Kluson, M. Drobek, S. Krejcikova, J. Krysa, A. Kalaji, T. Cajthaml, J. Rakusan, Appl. Catal. B: Environ. 80 (2008) 321–326.
[8] P. Kluson, M. Drobek, A. Zsigmond, J. Baranyi, P. Bata, S. Zarubova, A. Kalaji, Appl. Catal. B: Environ. 91 (2008) 51–59.
[9] P. Kluson, M. Drobek, A. Kalaji, S. Zarubova, J. Krysa, J. Rakusan, J. Photochem. Photobiol. A: Chem. 199 (2008) 267–273.
[10] M.P. Pond, B.B. Wenke, M.R. Preimesberger, S.L. Rice, J.T.J. Lecomte, Chem. Biodiv. 9 (2012) 1703–1717.
[11] M. Sugishima, Y. Kitamori, M. Noguchi, T. Kohchi, K. Fukuyama, J. Mol. Biol. 389 (2009) 276–387.
[12] P. Kluson, M. Drobek, T. Strasak, J. Krysa, M. Karaskova, J. Rakusan, J. Mol. Catal. A: Chem. 272 (2007) 213–219.
[13] T.B. Ogunbayo, E. Antunes, T. Nyokong, J. Mol. Catal. A: Chem. 334 (2011) 123–129.
[14] R. Gerdes, D. Wohrle, W. Spiller, G. Schneider, G. Schulz-Ekloff, J. Photochem. Photobiol. A: Chem. 111 (1997) 65–74.
[15] T.C. Oldham, D. Phillips, J. Photochem. Photobiol. B: Biol. 55 (2000) 16–19.
[16] K. Ozoemena, N. Kuznetsova, T. Nyokong, J. Photochem. Photobiol. A: Chem. 139 (2001) 217–224.
[17] B. Agboola, K. Ozoemena, T. Nyokong, J. Mol. Catal. A: Chem. 248 (2006) 84–92.
[18] K. Lang, J. Mosinger, D. Wagnerova, Chem. Listy 99 (2005) 211–221.
[19] J.H. Baxendale, J.A. Wilson, Trans. Farad. Soc. 16 (1995) 344–356.
[20] R. Andreozzi, V. Caprio, A. Insola, R. Marotta, Catal. Today 53 (1999) 51–59.
[21] Y. Ogata, K. Tomizawa, K. Takagi, Can. J. Chem. 59 (1981) 14–18.
[22] S. Guittonneau, J. de Laat, M. Dore, J.P. Duguet, C. Bonnel, Rev. Sci. Edu. 1 (1988) 35–54.
[23] O. Legrini, E. Oliveros, A.M. Braun, Chem. Rev. 93 (1993) 671–698.
[24] P. Kluson, M. Drobek, A. Kalaji, M. Karaskova, J. Rakusan, Res. Chem. Intermed. 35 (2009) 103–116.
[25] P. Zamostny, Z. Belohlav, Comput. Chem. 23 (1999) 479–485.
[26] L. Dusek, Chem. Listy 104 (2010) 846–854.
[27] E. Lipczynska-Kochany, R.J. Bolton, Environ. Sci. Technol. 26 (1992) 259–262.
[28] S. Antonaraki, E. Androulaki, D. Dimotikali, A. Hiskia, E. Papaconstantinou, J. Photochem. Photobiol. A: Chem. 148 (2002) 191–197.
[29] M. Hugül, R. Apak, S. Demirci, J. Hazard. Mater. B 77 (2000) 193–208.
[30] P.G. Tratnyek, V.G. Hoigne, Environ. Sci. Technol. 25 (1991) 1596–1607.
[31] M. Czaplicka, J. Hazard. Mater. 134 (2006) 45–59.